Stripe domains in a nearly homeotropic nematic liquid crystal: A bend escaped state at a nematic–smectic-*A* transition

V. M. Pergamenshchik,[1,2] I. Lelidis,[3,4] and V. A. Uzunova[2]
[1]*Display&Semiconductor Physics, Korea University, Jochiwon-eup, Yeongi-gun, Chungnam 339-700, South Korea*
[2]*Institute of Physics, Prospect Nauki 46, Kiev 03039, Ukraine*
[3]*Laboratoire de Physique de Systèmes Complexes, Université de Picardie Jules Verne, 33 Rue Saint-Leu, 80039 Amiens, France*
[4]*Solid State Section, Departement of Physics, University of Athens, Panepistimiopolis, Zografos, Athens 157 84, Greece*
(Received 10 December 2007; published 11 April 2008)

We report an observation and mechanism of spontaneous periodic modulations of the nematic director close to the temperature T_{NA} of a nematic-to-smectic-*A* phase transition if the surface alignment slightly differs from a pure homeotropic one. Stripe domains appear in the nematic phase about one degree above T_{NA} and persist into the Sm*A* phase. The instability of the homogeneous state with respect to stripe domains is shown to be related to a very large bend constant which is much larger than the twist and splay elastic constants. The instability mechanism consists of reduction of the highly energetic bend deformation, induced by small surface director tilts, at the expense of a spontaneous periodic splay-twist modulation. Using smallness of the twist-to-bend and splay-to-bend elastic constant ratios, the critical condition of the instability and the modulation period are found analytically. Both the experimentally obtained and theoretically predicted domain period scales very closely to a square root of the cell thickness.

DOI: 10.1103/PhysRevE.77.041703 PACS number(s): 61.30.Dk, 64.70.mf

I. INTRODUCTION

Formation of patterns of the director field under the action of an external force is an important macroscopic property of liquid crystalline phases. A fundamental property of liquid crystals (LCs) that derives from their unique elastic properties is that in many geometries patterns appear spontaneously, i.e., their symmetry is lower than the symmetry of the force applied to the sample. On the macroscopic level, there are two essentially different groups of static mechanisms behind a possible spontaneous pattern formation in a nematic LC: the one related to the divergence elasticity and the one due to the appreciable elastic anisotropy related to a difference between the splay, twist, and bend elastic constants [1].

The divergence elastic mechanisms of a spontaneous pattern formation originates from the fact that the divergence elastic K_{24} (saddle-splay) and K_{13} terms are not positive definite which reflects the intrinsic ability of the system to gain energy at the expense of finite deformations. The divergence elasticity can induce spontaneous patterns both in the presence of an external torque applied to the director [3,4] and without any external forces, i.e., just in the homogeneous ground state [5–8].

The elastic anisotropy is associated with the positive definite K_{11} (splay), K_{22} (twist), and K_{33} (bend) elastic terms, which describe the resistance of a nematic system to any director deformations. Therefore these terms cannot cause a spontaneous pattern formation from the uniform ground state, and an external torque must necessarily be present. The symmetry breaking can occur because the three independent elastic deformation modes, the splay, twist, and bend, cost different energy. If an external torque induces one of these mode while the system can reduce the energy at the expense of a spontaneously produced less energetic mode, then both the former mode reduces and the latter appears. As the second, the spontaneous mode is more complicated and has the symmetry lower than that dictated by the external force, this instability results in a spontaneous symmetry breaking. It is clear that such an instability strongly depends on how large the energy difference between different modes is, i.e., how strong the elastic anisotropy is. A well-known example of such an effect is the stripe Frederiks transition [9]. A homogeneous magnetic field applied to a homogeneous planar nematic layer can produce a single homogeneous mode, the splay Frederiks mode homogeneous in the layer plane. However, if the splay-twist elastic anisotropy is sufficiently strong, the energy can be reduced by spontaneous twist deformations, periodic in the layer plane, and the in-plane homogeneity turns out to be spontaneously broken. This instability is possible only if the twist mode is considerably less energetic than the splay mode, $K_{22}/K_{11}<1/3$ [10–12], which can be achieved only in some polymer-related nematic LCs (for standard nematics $K_{22}/K_{11}\sim 0.5$).

However, as the K_{24} term and the energy saving twist term are proportional to $\sin^2\theta$ where θ is the director tilt with respect to the layer normal, both mechanisms described above are inefficient in a homeotropic geometry where $\theta=0$. Moreover, even for a finite but modest tilt, θ^2 is still small and spontaneous formation of static patterns in geometries close to a homeotropic one is highly hindered. This situation can be changed only if the small θ^2 is compensated by very large values of some elastic constants, i.e., by a very strong elastic anisotropy. The only possibility to have an anomalously large elastic anisotropy in a nematic LC is to work with mesogens, that have a Sm*A* phase, close to the temperature T_{NA} of a nematic–Sm*A* transition. It is known that in a close vicinity of a Sm*A* phase the twist and bend elastic constants of a nematic LC become large (formally speaking, they diverge at T_{NA}), while the splay constant remains of the standard magnitude [13–15]. This offers an interesting possibility to study spontaneous pattern formation under the extreme conditions when the elastic ratios b

$=K_{33}/K_{11}$, $t=K_{22}/K_{11}$, $b/t=K_{33}/K_{22}$, and K_{24}/K_{11} are anomalously large. In the planar geometry or geometry with the large angle θ, spontaneous periodic patterns at T_{NA} had been observed decades ago [12,16,17] (nowadays the problem still remains attractive, see, e.g., [6]). At last, recently observations of spontaneous periodic patterns at T_{NA} had also been reported in a homeotropic geometry.

The authors of [18] observed a periodic Frederiks transition from a homeotropic state, induced by a slightly oblique electric field. More recently, a novel periodic structure, which spontaneously appears at a nematic–Sm*A* transition in a field-free geometry close to homeotropic, was reported in Ref. [19]. Approaching the Sm*A* phase from the nematic phase, slightly above T_{NA}, periodic domains were observed in restricted islandlike areas of a homeotropic cell where their appearance followed a homeotropic-small tilt anchoring transition. These areas appeared after a surface treatment, and we could not control their location, size, and even their very existence; at most, such islands contained 15–20 stripes. Below T_{NA} both the pretilt and stripes almost immediately disappeared, and in the Sm*A* phase only a homogeneous homeotropic texture was observed. As it was not clear what was the role of the finite size and shape of the stripe islands and the walls separating them from the homogeneous homeotropic surrounding, the nature of this effect remained unclear. Motivated by this, we attempted to produce homogeneous almost homeotropic nematic layers with a small pretilt and explore a potential pattern formation when the temperature is in the vicinity of T_{NA}. In this paper we report results of this study and present theory of the effect observed.

We observed a spontaneous periodic director modulation in a homogeneous almost homeotropic layer with a small pretilt. Regular stripes appeared in the nematic phase of a compound *4-octyloxyphenyl-4'-pentyloxybenzoate* close to T_{NA}, but, surprisingly, they persisted deeply into the Sm*A* phase. The period L was measured as a function of the layer thickness H. We also present an analytical theory of the effect which is exact in the leading order in the small parameters $1/b$, t/b, and θ^2. The spontaneous stripe modulation is shown to occur due to the high splay-bend and twist-bend elastic anisotropy. The critical condition for the instability to occur contains the elastic ratios b and t, the pretilt angles on the layer's surfaces, the ratio h of the layer thickness H to the polar anchoring extrapolation length $L_{11}=K_{11}/$(polar anchoring W), and the ratio w_a of the azimuthal anchoring to the polar anchoring W. The modulation period is found to scale as a square root of the thickness which is in good agreement with the experiment.

II. EXPERIMENTAL RESULTS

The liquid crystal cell is made up of two flat glass plates treated with *n,n-dimethyl-n-octadecyl-3-aminopropyltrimethoxysilyl-chloride* (DMOAP) to induce homeotropic alignment [20]. After cleaning, the glass plates were covered with a thin DMOAP film by dipping them in a stirred dilute solution. Finally, the plates were rinsed with distilled water and dried at 110 °C for 1 h under a nitrogen atmosphere. The thickness of the cell was measured either by focusing at the two glass plates or by using mylar spacers.

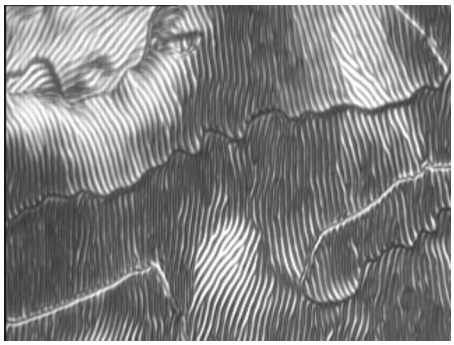

FIG. 1. Stripe texture in a layer of *4-octyloxyphenyl-4'-pentyloxybenzoate* at the temperature slightly above the nematic–Sm*A* transition in an initially almost homeotropic cell. The cell thickness $H=1.8$ μkm, the period $L=6.6$ μm.

The LC compound used in this work is *4-octyloxyphenyl-4'-pentyloxybenzoate*. It exhibits the following transitions: isotropic $\rightarrow$ nematic at $T_{NI}=85$ °C, nematic $\rightarrow$ Sm*A* at $T_{NA}=66$ °C, Sm*A* $\rightarrow$ Sm*C* at 64 °C, and Sm*C* $\rightarrow$ crystal at 58 °C. The cell was enclosed in a hot stage (Instec mK) providing the temperature stability 0.01 °C. The LC compound was introduced between the plates by capillarity in the isotropic phase. The observations were done with a polarized-light microscope in the transmission mode.

When cooling the sample from the isotropic to nematic phase, we observed appearing of almost homeotropic domains with a small tilt. The domains are separated by splay-bend π-walls across which the in-plane director projection turns by about π and the tilt changes its sign. Recurring the sample by heating it to the no-tilt state and cooling back to the tilt state does not change the optical landscape in general, but does not reproduce the previous domain patterns exactly. This variation of the tilt direction from one domain to another indicates a degeneracy of the azimuthal easy direction and thus weak azimuthal anchoring (the surfaces were not treated as to induce an azimuthal easy direction). We have never obtained a uniform homeotropic alignment: the tilt in different domains is slightly different. The tilt of $\mathbf{n}$, estimated by the phase retardation technique [21], varies around the mean value $\sim 6° - 10°$. It is known that this standard technique gives the average tilt $(\theta_2+\theta_1)/2$, where θ_2 and θ_1 are tilt angles at the two layer surfaces, and the hybridity $\theta_2 - \theta_1$, if any, cannot be detected by this technique [22].

When the temperature is further lowered toward the nematic–Sm*A* transition temperature T_{NA}, a transition from the uniform tilt structure to a stripe state occurs at some T_c which is slightly above T_{NA}. The small difference $T_c - T_{NA}$ varies for different cells, but it has not been possible to establish a certain tendency. The obvious reason is that the cells' parameters, and, most importantly, the pretilt which varies even from domain to domain in the same sample, cannot be controlled with the accuracy corresponding to the very subtle difference in $T_c - T_{NA}$. The stripes always appear in the entire sample of a surface area ≈ 2 cm^2.

Figure 1 shows a typical observed striped texture in a 1.8 ± 0.2 μm thick cell which is nearly uniform in the entire

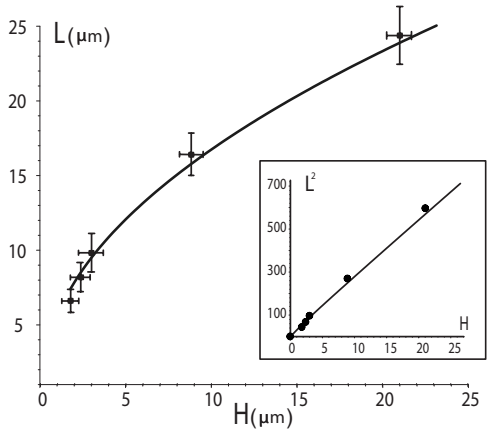

FIG. 2. Experimental stripe period L vs cell thickness H (symbols). The solid curve represents theoretical fits which are practically indistinguishable for all of the curves in Fig. 3. Inset shows that $L^2(H) \propto H$ and thus $L(H)$ is very close to $L(H) \propto \sqrt{H}$.

sample. The period L of the stripes is $L=6.6\pm0.2$ μm. No apparent dependence of the stripe period on the temperature has been detected: once the stripes have appeared their period remains unchanged while the stripes exist. The stripes are sharply defined by a strong optical contrast. We have not found any twist deformation in the stripe texture. Experimentally, we identify the stripes as domains of a splay-bend texture with the nematic director periodic in the direction perpendicular to the stripes. Finally, we note that the striped texture persists into the temperature range of the SmA phase without any apparent period variation until it vanishes at some temperature below T_{NA}.

Figure 2 gives a plot of the measured period L of the stripe texture as a function of the cell thickness H. The inset shows that the experimental data $L^2(H)$ fall fairy well onto the curve $L^2 \propto H$, and thus $L \propto \sqrt{H}$.

The domains with different tilts are separated by the same splay-bend walls which separate the domains with different tilts before the stripe modulation has developed, see Fig. 1. Along with the fact that the domains include many periods of the modulation this implies that the domain shape is not connected to the modulation structure except at the close proximity of the domain boundary. An important observation has been that the width ℓ_d of these walls remains nearly constant of the order of a few micrometers for all temperatures. Valuable information about relative strength of the elasticity and anchoring can be obtained from this result in the context of the well- known relation $W \approx KH(\delta\theta/\ell_d)^2/2$, where K is the elastic constant, H is the cell thickness, and $\delta\theta$ is the reorientation angle across the wall [23]. Well above T_{NA} the elastic constant is known to be $K \sim 10^{-11}$ N, and thus the polar anchoring can be estimated as $\sim 10^{-5}$ J/m^2 [20,23] and the extrapolation length $K/W \sim 1$ μm. At temperatures close to T_{NA}, where neither K nor W is known, one obtains the relation $K/W \approx 2/H(\delta\theta/\ell_d)^2$, which tells us that the ratio (bend elastic constant)/(polar anchoring) ~ 1 μm and is temperature independent. Below we will see that this relation has an important implication in the context of our theoretical interpretation of the experimental findings.

As the periodic patterns appear in a nematic phase above T_{NA}, the onset of the modulation can be fully described in terms of the nematic free energy (FE). The patterns, however, do not change much while existing in a short interval of temperatures below T_{NA}. This shows that the periodically distorted sample remains in a kind of nematic phase even somewhat below T_{NA}. Indeed, as shown in Ref. [6], in a nematic phase with director deformations the temperature of the transition to SmA is lower than the standard transition temperature T_{NA} in a spatially homogeneous state. For sufficiently low temperature, however, the smectic layering suppresses the deformation, the periodic modulation disappears, and the SmA phase occurs.

III. THEORY

A. General formulas and statement of the problem

As the instability occurs in a nematic phase and the domain periodicity L, once it has appeared, does not change in the whole of the temperature range of its existence, our task is to describe this onset of the instability of the nematic director. The theory has to answer when the homogeneous deformation [homogeneous state (HS)], which is induced by small surface tilts and depends on a single coordinate normal to the layer, becomes unstable with respect to a periodic modulation [domain state (DS)].

The total FE F associated with the nematic director $\mathbf{n}$ is the sum of the deformation FE F_d and anchoring FE F_a, i.e., $F=F_d+F_a$. The FE of director deformations has the form

$$F_d = \frac{K_{33}}{2}\int dV\left\{\frac{1}{b}(\nabla\cdot\mathbf{n})^2 + \frac{t}{b}(\mathbf{n}\cdot\nabla\times\mathbf{n})^2 + (\mathbf{n}\times\nabla\times\mathbf{n})^2 - 2(K_{24}/K_{33})\,\nabla\cdot[\mathbf{n}(\nabla\cdot\mathbf{n}) + \mathbf{n}\times\nabla\times\mathbf{n}] + 2(K_{13}/K_{33})\,\nabla\cdot[\mathbf{n}(\nabla\cdot\mathbf{n})]\right\} \quad (1)$$

(the dimensionless constants b and t were introduced above). Along with the three positive definite splay, twist, and bend terms which resist any deformations, F_d contains two sign indefinite divergence K_{24} and K_{13} terms. The elastic theory predicts that only four constants are independent since [2,24]

$$K_{24}/K_{11} = \frac{1}{4}(1+t). \quad (2)$$

The anchoring energy consists of the polar anchoring that gives the energy of the surface director deviation from the out-of-surface, polar easy direction, and the azimuthal anchoring that gives the energy of deviation of the in-surface director component from the in-surface, azimuthal easy direction. In our case the polar easy axis on the upper ("2") and lower ("1") layer surface are almost homeotropic, i.e., tilted by a small angle $\bar{\theta}_2$ and $\bar{\theta}_1$, respectively. For simplicity we assume $\bar{\theta}_2=\bar{\theta}$ and $\bar{\theta}_1=0$. The azimuthal easy directions on both surfaces coincide. When the director deviations from the easy axes are small, the anchoring potentials are well-represented by the Rapini-Popoular form which will be assumed in our calculations.

Consider a plane nematic layer of thickness H in the reference frame with the coordinate z which is normal to the

layer and has the onset $z=0$ on its lower surface "1." We use the standard director parametrization $\mathbf{n}=(\sin\Theta\cos\phi,\sin\Theta\sin\phi,\cos\Theta)$ by the polar angle Θ counted from the z axis, and the azimuthal angle ϕ counted from the x axis. Variables related to the upper surface $z=H$ and lower surface $z=0$ will be indicated by subscripts 2 and 1, respectively. Then the anchoring energy can be represented as the following surface integral:

$$F_a=\frac{W}{2}\int dxdy[\sin^2\Theta_1+w_p\sin^2(\Theta_2-\bar{\theta}) + w_{a1}\sin^2\Theta_1\sin^2\phi_1+w_{a2}\sin^2\Theta_2\sin^2\phi_2], \quad (3)$$

where W is the polar anchoring coefficient on the surface 1, while that on the surface 2 is w_pW; the azimuthal anchoring coefficients are $w_{a2}W\Theta_2^2$ and $w_{a1}W\Theta_1^2$, the azimuthal easy direction is along the x axis. The azimuthal anchoring depends on the square $\sin^2\Theta$ of the in-plane projection of the director: if the director is normal to the surface there is no in-plane anisotropy, whereas it is maximum when the director lies in the plane.

For convenience we now introduce the following dimensionless quantities: the reduced coordinates z/H and y/H for which we retain the same notations z, $0\le z\le 1$, and y; reduced thickness $h=H/L_{11}$ where $L_{11}=K_{11}/W$ is the anchoring extrapolation length for the lower surface "1"; FE's F, F_{HS}, and F_2 in units $K_{33}/4H$.

In a homeotropic geometry the polar anchoring strength W is known to rapidly grow in the proximity of a nematic–SmA transition because of the nascent surface layering and at T_{NA} can be as large as 10^{-3} J m^{-2} [25]. As a result, the extrapolation length L_{11}, which is of the order of a micrometer a few degrees above the transition, at T_{NA} can dramatically decrease to values of order 10^{-2} μm or smaller. Therefore the reduced thickness h can be ~ 100 even when the actual thickness $H\sim 1$ μm. At the same time, the azimuthal anchoring, which is not expected to change appreciably, will be assumed to be always very weak.

In terms of the parametrizing angles the HS director $\mathbf{n}_{HS}$ is given by $\Theta=\theta(z)$, $\phi=0$, i.e.,

$$\mathbf{n}_{HS}(z)=(\sin\theta,0,\cos\theta). \quad (4)$$

The function $\theta(z)$ is a minimizer of the functional

$$F_{HS}=2\int_0^1 dz\left(\frac{1}{b}\sin^2\theta+\cos^2\theta\right)\theta'^2 + \frac{2h}{b}[w_p\sin^2(\theta_2-\bar{\theta})+\sin^2\theta_1], \quad (5)$$

which is the FE of the HS per unit length in the y direction; here and below the prime over the variable stands for the z derivative.

In the DS, $\mathbf{n}$, the director $\mathbf{n}_{HS}$ of the HS is weakly perturbed, $\mathbf{n}=\mathbf{n}_{HS}+\delta\mathbf{n}$. The perturbation $\delta\mathbf{n}$ is periodic along the y axis and independent of x:

$$\Theta=\theta(z)+f(z)\sin(\chi y),$$

$$\phi=g(z)\cos(\chi y), \quad (6)$$

where $\chi=2\pi H/L$ is the dimensionless wave number and L is the period along the y axis. The energy F per unit length along y of the DS in the leading (quadratic) order in the small amplitudes f and g is given by the sum

$$F\{\mathbf{n}\}\simeq F_{HS}\{\mathbf{n}_{HS}\}+F_2\{\mathbf{n}_{HS},\delta\mathbf{n}\}, \quad (7)$$

where F_2 is the second variation in $\delta\mathbf{n}$ of the total energy F about the HS director $\mathbf{n}_{HS}$. Analysis of the instability of the HS performed below shows that it requires the elastic anisotropy to satisfy the inequality

$$1/b<t/b\ll 1. \quad (8)$$

The same conclusion was achieved by the authors of [18] considering a field-induced instability of a homeotropic state at T_{NA}. Relation (8) is consistent with the experimental results on the elastic anisotropy of a compound 8CB at T_{NA} [26] and was used for theoretical analysis of the periodic Frederiks transition far from a homeotropic state in [12]. We also assume that the elastic anisotropy is of the kind described by the inequality (8) which will be justified *a posteriori*. Therefore in F_2 we omit the terms $\sim 1/b$ (in particular, the K_{13} term), but, at the same time, terms $\sim t/b$ and $\sim h/b$ might be not negligible since t and h can be large, and we retain them. Another simplification derives from the smallness of θ and allows for expanding $\mathbf{n}_{HS}$ in θ and restricting F_2 to the order $O(\theta^2)$. Then, after the y integration, the functional F_2 obtains in the form

$$F_2=\int_0^1 dz\left[f'^2-4\theta\theta' ff'+\left(\frac{t}{b}\chi^2-\theta'^2\right)f^2+\theta^2g'^2 + 2\chi\theta\theta' gf+\frac{2t\chi\theta^2fg'}{b}+\frac{\theta^2\chi^2g^2}{b}\right]+\frac{2p_{\|}\chi}{b}(\theta_2^2f_2g_2 - \theta_1^2f_1g_1)+\frac{h}{b}(w_pf_2^2+f_1^2+w_{a2}\theta_2^2g_2^2+w_{a1}\theta_1^2g_1^2), \quad (9)$$

where $p_{\|}=(K_{11}-2K_{24})/K_{11}=(1-t)/2$ is the total reduced saddle-splay constant (cf., see Refs. [2,4–6]); the bulk term of order $\theta^2f'^2\ll f'^2$ and the anchoring terms $\sim\bar{\theta}^2f^2\ll f^2$ are neglected.

The functional F_2 is the FE of periodic modulations. If the modulation can be such that $\min F_2<0$, the HS becomes unstable, and the modulation with nonzero amplitudes f and g appears. The critical condition for this instability to occur is $\min F_2=0$. Thus minimization of the functional $F_2\{f,g\}$ is now in order. To this end we first find the angle $\theta(z)$ which determines the HS.

B. Homogeneous state

Here we minimize the functional F_{HS} (5) to determine the HS $\theta(z)$. Omitting the term $\frac{1}{b}\sin^2\theta\ll\cos^2\theta$ in the functional F_{HS} and the term $\sin\theta\theta'^2\ll\cos\theta\theta''$ in its Euler-Lagrange equation, one has

$$\theta''=0. \quad (10)$$

This equation has the solution

$$\theta = \Delta z + \theta_1, \tag{11}$$

where Δ and θ_1 are integration constants. The boundary conditions to the Euler-Lagrange Eq. (10) have the form

$$\cos^2\theta_2\theta_2' + \frac{w_p h_b}{2}\sin 2(\theta_2 - \bar{\theta}) = 0,$$

$$\cos^2\theta_1\theta_1' - \frac{h_b}{2}\sin 2\theta_1 = 0, \tag{12}$$

where $h_b = h/b$. Making use of Eq. (11) and the smallness of $\theta's$, this system goes over into

$$\Delta + w_p h_b(\Delta + \theta_1 - \bar{\theta}) = 0,$$

$$\Delta - h_b\theta_1 = 0. \tag{13}$$

The solution of this system is

$$\theta_2 = \frac{w_p\bar{\theta}(1+h_b)}{1 + w_p + w_p h_b},$$

$$\theta_1 = \frac{w_p\bar{\theta}}{1 + w_p + w_p h_b}. \tag{14}$$

From Eqs. (14) we obtain the quantity Δ which enters $\theta(z)$ [Eq. (11)] and represents hybridity of the HS, i.e.,

$$\Delta = \theta_2 - \theta_1 = \frac{w_p h_b\bar{\theta}}{1 + w_p + w_p h_b}. \tag{15}$$

C. Minimization of the FE of the domain state

A straightforward minimization of the functional F_2 is highly laborious and does not allow for a clear interpretation of the intermediate algebra. At the same time, the result can be obtained on the grounds of following clear and simple considerations. First, we notice that the coefficient of the positive bend term f'^2 is much larger than all other coefficients in Eq. (9), hence the FE is minimized by f independent of z: f=const and f'^2=0. Second, it is not difficult to see that the minimum of F_2 also favors g independent of z. Indeed, F_2 has three sign indefinite terms which, at least in principle, can favor the modulation. These are the bulk terms $2\chi\theta\theta' gf$ and $2(t/b)\chi\theta^2 fg'$, and the surface term with the coefficient $2(p_\parallel/b)\chi$ [the terms without χ and g have no connection to the y-dependent modulation, their sum is positive as the HS solution, Eqs. (11) and (14), is the minimizer of F_{HS} if the perturbation depends solely on z]. Clearly, by virtue of Eqs. (8) and (2), the first of these terms is much larger in its magnitude than the other two, and thus it is this term $2\chi\theta\theta' gf$ which drives the modulation. On the one hand, this term is finite for a z-independent g while, on the other hand, a z-dependence of g would result in a finite (and large) positive term $\theta^2 g'^2$. This implies that the instability is favored by z independent of g [which is also consistent with the fact that the twist deformation ($\propto g'$) is not observed experimentally]. Thus F_2 is minimized by f and g independent of z. Notice that under this condition, the term $\int_0^1 dz 2\chi\theta\theta' gf = \chi(\theta_2^2 - \theta_1^2)gf \propto \Delta$, so that a finite hybridity Δ is necessary for the instability to occur.

We now introduce a number of auxiliary quantities which will appear in the forthcoming formulas. These quantities, which depend on the elastic and anchoring constants, the surface angles θ_1 and θ_2, and hybridity Δ, are defined as

$$w_a = w_{a1}\theta_1 + w_{a2}\theta_2,$$

$$p = 1 - 2p_\parallel/b,$$

$$S_1 = \frac{\Delta^2}{3} + \theta_1\theta_2,$$

$$S_2 = h_b(1 + w_p) - \Delta^2. \tag{16}$$

Then, the functional F_2 goes over into the following quadratic form of constant f and g:

$$F_2 = Af^2 + Bg^2 - 2Cfg. \tag{17}$$

where

$$A = \frac{t}{b}\chi^2 + h_b(1 + w_p) - \Delta^2,$$

$$B = \frac{\chi^2}{b}\left(\frac{\Delta^2}{3} + \theta_1\theta_2\right) + h_b w_a,$$

$$C = \frac{\chi}{2}p\Delta(\theta_1 + \theta_2). \tag{18}$$

The onset of the instability is given by the condition $\min F_2 = 0$ which is equivalent to the equality $AB - C^2 = 0$. It can be reduced to the following form:

$$\alpha\chi^4 + \beta\chi^2 + \delta = 0, \tag{19}$$

where

$$\alpha = \frac{t}{b^2}S_1,$$

$$\beta = \frac{1}{b}S_1 S_2 - \frac{p^2}{4}\Delta^2(\theta_1 + \theta_2)^2 + \frac{t}{b}h_b w_a,$$

$$\delta = h_b w_a S_2. \tag{20}$$

The quantities α, β, and γ depend on b both explicitly and via the b-dependent $S's$, $\theta's$, w_a, and h_b. Consider the solution of Eq. (19),

$$\chi^2 = \frac{-\beta \pm \sqrt{\beta^2 - 4\alpha\delta}}{2\alpha}. \tag{21}$$

It is seen from Eqs. (20) and (16) that $\alpha > 0$ and $\delta > 0$. Hence to get $\chi^2 > 0$ we need b to satisfy the two conditions: $D(b) = \beta^2 - 4\alpha\delta \geq 0$ and $\beta(b) \leq 0$. The explicit dependence of $D(b)$ on b is quadratic with the positive coefficient of b^2. This quadratic form has two roots, b_- and b_+, $b_- < b_+$, given by the formula

$$b_{\pm}(b) = \frac{4(\sqrt{S_1 S_2} \pm \sqrt{t h_b w_a})^2}{p^2 \Delta^2 (\theta_1 + \theta_2)^2}. \quad (22)$$

Then the inequality $D(b) \geq 0$ is satisfied provided there takes place any of the following two inequalities: $b \leq b_-$ or $b \geq b_+$. In turn, the inequality $\beta(b) \leq 0$ under the necessary condition $\Delta \neq 0$ reduces to $b \geq b_0$ where

$$b_0(b) = \frac{4(S_1 S_2 + t h_b w_a)}{p^2 \Delta^2 (\theta_1 + \theta_2)^2}. \quad (23)$$

Since $b_- \leq b_0 \leq b_+$, we have $\chi^2 \geq 0$ when $b \geq b_+ = b_+(b_c)$. Thus the critical value of $\chi_c = \chi(b_c)$ is obtained (numerically) from the equation

$$b_c = b_+(b_c) \quad (24)$$

(if $\Delta \to 0$, then b_+ diverges which again shows that the hybridity Δ must be sufficiently large). Since this equation implies $D(b_c) = 0$, Eq. (21) reduces to $\chi_c^2 = \sqrt{\delta(b_c)/\alpha(b_c)}$. Making use of the definition (20) of δ and α, for the reduced wave number of the DS one obtains the formula

$$\chi_c = \left(\frac{h_b w_a S_2 b^2}{t S_1} \right)^{1/4}_{b=b_c(h)}, \quad (25)$$

in which $\theta_1(b,h)$ and $\theta_2(b,h)$ are determined solely by the HS, Eq. (14). The domain period is calculated as $L = 2\pi H/\chi_c$ and, when expressed in terms of the actual thickness H, obtains in the form

$$L = 2\pi \sqrt{L_{11} H} \left[\frac{t(\theta_2^2 + \theta_1^2 + \theta_1 \theta_2)}{3(1 + w_p - b\Delta^2 L_{11}/H)(w_{a1}\theta_1 + w_{a2}\theta_2)} \right]^{1/4}_{b=b_c(h)}. \quad (26)$$

As θ_2 and θ_1 as well as the critical value of b depend on the reduced thickness $h = H/L_{11}$, in principle, χ_c and L depend on H in a more complicated manner than just that given by the factor $\sqrt{H}$. However, the numerical results discussed below show that actually $L \propto \sqrt{H}$ with a high accuracy.

IV. RESULTS AND DISCUSSION

The physical picture developed above can be described as follows. As temperature of the sample is approaching a close proximity of T_{NA}, the elastic constant ratios b and t start to grow fast and take the values described by the inequality (8). The homeotropic-to-tilt surface transition occurs after which the director tilt is homogeneous in the layer plane. The homogeneous pretilt is different at the lower and upper surface so that there is a small hybridity $\Delta = \theta_2 - \theta_1$. On further cooling, the temperature attains some critical value $T_c \gtrsim T_{NA}$ for which the ratio $b_c = b(T_c)$ and thus the energy price for the hybridity is so large that the system becomes unstable with respect to a periodic modulation. This modulation saves the energy by decreasing the bend deformation at the expense of producing the DS with periodic splay and twist deformations. The period L of the DS remains equal to its value at b_c with which the domains first appear at T_c, as after that their size is frustrated by the boundary conditions at the sample's periphery.

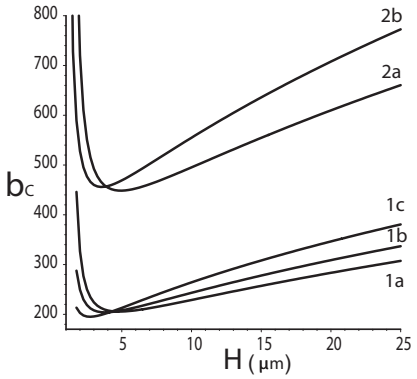

FIG. 3. Critical values of the bend elastic ratio b_c vs layer thickness H, calculated from Eq. (24) for $w_p = 1.2$, $\bar{w}_a = w_{a1} = w_{a2}$, and the following parameters. Curve 1a: $\bar{\theta} = 0.3$, $t = 6$, $L_{11} = 0.015$ μm, and $\bar{w}_a = 5 \cdot 10^{-4}$; curve 1b: $\bar{\theta} = 0.3$, $t = 10$, $L_{11} = 0.012$ μm, and $\bar{w}_a = 5 \cdot 10^{-4}$; curve 1c: $\bar{\theta} = 0.3$, $t = 20$, $L_{11} = 0.009$ μm, and $\bar{w}_a = 5 \cdot 10^{-4}$; curve 2a: $\bar{\theta} = 0.2$, $t = 6$, $L_{11} = 0.007$ μm, and $\bar{w}_a = 10^{-4}$; and curve 2b: $\bar{\theta} = 0.2$, $t = 20$, $L_{11} = 0.005$ μm, and $\bar{w}_a = 2 \cdot 10^{-4}$.

Mathematically, the energy decrease in the DS is described by the FE density $2\chi\theta\theta' gf$ which drives the instability. For z independent perturbations f and g, which favor the DS, this term is a total derivative and, after the bulk integration, goes over into $\chi(\theta_2^2 - \theta_1^2) gf$. This shows that a finite hybridity Δ is a necessary precondition for the instability. The critical value b_c is found from the equation $b_c = b_+(b_c)$ (24) which contains the normalized reduced thickness $h_b = (H/L_{11})/b$, the elastic ratio t, and the polar and azimuthal anchoring coefficients w_p, w_{a1}, and w_{a2} as parameters, hence $b_c = b_c(H/L_{11}, \bar{\theta}, t, w_p, w_{a1,2})$. When b_c is found for fixed values of these parameters, the period $L(H)$ can be calculated from formulas (26) and (14).

Dependence of the critical elastic ratio b_c on the other parameters was obtained by solving the irrational algebraic equation $b_c = b_+(b_c)$ numerically, Fig. 3. The values of the parameters L_{11}, t, w_p, and $\bar{w}_a = w_{a1} = w_{a2}$ were chosen as to provide the fit to the experimental data and, at the same time, to keep $\bar{\theta}$ and b_c at possibly low values. All of the curves in Fig. 3 give equally good and practically indistinguishable fits to the experimental data, Fig. 2, if the extrapolation length L_{11} is chosen as indicated in the caption to Fig. 3. These values of $L_{11} \sim 0.005$–0.015 which is in accord with the values of a polar anchoring W generally expected at a nematic–SmA transition [25] [see discussion above Eq. (4)]. The clear trend is that a smaller $\bar{\theta}$ requires a larger b_c. The curves in Fig. 3 demonstrate how large b_c should be if the tilt is induced by the easy direction $\bar{\theta} = 0.3$ and 0.2: for these tilts the DS appears for the bend elastic ratio b_c of the order of hundreds. One can see that the critical value of b_c correlates with the temperature-dependent anchoring extrapolation length L_{11}: a higher b_c is accompanied by a smaller L_{11} so that $b_c L_{11} = K_{33}/W$ always remains close to 1 μm which is the extrapolation length K_{11}/W well above T_{NA}. Thus the ratio $K_{33}(T)/W(T) \approx 1$ μm is nearly independent of temperature which is in a qualitative accord with our experimental findings. This is a natural result as the increase of anchor-

ing in a Sm*A* is actually an elastic phenomenon and expresses the fact that a surface tilt costs a high bend and twist elastic energy [25]. At the same time, the twist elastic ratio t is found to be considerably lower than b, i.e., in the range of tens: for a larger t the fit becomes poor. For a more quantitative discussion one needs experimental data on the behavior of the anchoring and bend and twist elastic ratios slightly above a nematic–Sm*A* transition, which, however, are both scant and nonconclusive (see discussion in [13,14]). The only known experimental temperature dependence of anchoring at T_{NA} [25], $W \sim W_{NA} + 0.09(1 - T/T_{NA})^{0.65 \pm 0.09}$ with $W_{NA} \sim 10^{-3}$ J/m^2, is measured in the Sm*A* phase, i.e., below T_{NA}. At the same time, the experimental data on 8CB obtained in [26] and parametrized in [12] as $b \sim (T/T_{NA} - 1)^{-0.7}$ and $t \sim (T/T_{NA} - 1)^{-0.35}$, show that t scales as $b^{1/2}$, which is in a qualitative agreement with the results obtained from our fit. The fact that the reciprocal to the exponent of $W(T)$ is close to that of $b(T)$ might be indicative of the reason why the ratio $K_{33}(T)/W(T)$ is almost temperature independent. This both supports our result and throws additional light on the problem of anchoring and elastic bend and twist moduli in a Sm*A*.

The azimuthal anchoring $\bar{w}_a W$, which provides the fit, is very small, $\bar{w}_a \sim 10^{-4} - 10^{-3}$. In other situations such a small azimuthal anchoring could have been merely set to zero, but at a nematic–Sm*A* transition with its specific interplay of the large and small numbers, this small but nonzero value is essential as $\bar{w}_a = 0$ results in $L = \infty$. The inset in Fig. 2 shows that the thickness dependence of the DS period is practically $L(H) \propto \sqrt{H}$ which is in accord with the experimental data.

The mechanism of the instability of the HS with respect to the DS requires a finite hybridity Δ (in our case $\Delta \lesssim \bar{\theta}$). We believe that a similar mechanism is responsible for the periodic patterns observed in [18]. These patterns were induced by an electric field in a homeotropic geometry slightly above the nematic–Sm*A* transition temperature of 8CB (the dielectric anisotropy is positive). The transition to the periodic state, described by the authors of [18], has a threshold. At the same time, as mentioned in [18], the electric field driving the transition is produced by two electrodes, placed on just one sample's surface, and thus is neither exactly parallel to the nematic layer nor symmetric with respect to its midplane. Such a field gives rise to a hybrid director alignment before the periodic instability. Indeed, it induces a thresholdless homogeneous (i.e., solely z-dependent) director tilt different at both surfaces. This hybridity of the homogeneous director distortions, which is gradually growing when the field strength is increasing from zero, precedes the transition to the periodic state which occurs at some threshold field. We see that the transition to DS observed in [18] starts from the homogeneous state with a finite hybridity, and the situation seems to be essentially similar to the one responsible for the periodic modulation in our field free case.

The general formula for the FE of the perturbation in the vicinity of a homeotropic state and, in particular, our Eq. (9), shows that a pure homeotropic state is stable with respect to any continuous instabilities (second order transitions) as the second order energy variation vanishes for $\theta = 0$. Here we have found that the situation does not change for a (small) pretilt if the surface tilts are equal: a final hybridity is necessary for an instability to occur in geometries close to the homeotropic one. This shows that the developed hybridity-related mechanism is quite general for instabilities of a nearly homeotropic state of the nematic director.

ACKNOWLEDGMENT

V.M.P. and I.L. gratefully acknowledge support of this work by the "Université de Picardie Jules Verne." V.M.P. also acknowledges support by grant F0004130-2007-23 from the Information Display R&D Center, One of the 21st Century Frontier R&D Program funded by the Ministry of Commerce, Industry and Energy of the Korean Government.

[1] On the microscopic level, both the finite divergence terms and the finite elastic anisotropy have the same origin, anisotropic fraction in the intermolecular interaction [2].
[2] V. M. Pergamenshchik and S. B. Chernyshuk, Phys. Rev. E **66**, 051712 (2002).
[3] G. P. Crawford and S. Žumer, Int. J. Mod. Phys. B **9**, 2469 (1995).
[4] O. D. Lavrentovich and V. M. Pergamenshchik, Int. J. Mod. Phys. B **9**, 2389 (1995).
[5] V. M. Pergamenshchik, Phys. Rev. E **61**, 3936 (2000).
[6] G. Barbero and V. M. Pergamenshchik, Phys. Rev. E **66**, 051706 (2002).
[7] G. Barbero, I. Lelidis, and A. K. Zvezdin, Phys. Rev. E **67**, 061710 (2003).
[8] G. Barbero, L. R. Evangelista, and I. Lelidis, Phys. Rev. E **67**, 051708 (2003).
[9] F. Lonberg and R. B. Meyer, Phys. Rev. Lett. **55**, 718 (1985).
[10] E. Miraldi, C. Oldano, and A. Strigazzi, Phys. Rev. A **34**, 4348 (1986).
[11] U. D. Kini, J. Phys. (Paris) **47**, 693 (1986).
[12] D. W. Allender, R. M. Hornreich, and D. L. Johnson, Phys. Rev. Lett. **59**, 2654 (1987).
[13] S. Chandrasekhar, *Liquid Crystals* (Cambridge University, New York, 1977).
[14] P. G. de Gennes and J. Prost, *The Physics of Liquid Crystals* (Clarendon, Oxford, 1993).
[15] M. Kleman and O. D. Lavrentovich, *Soft Matter Physics. An Introduction* (Springer, New York, 2003).
[16] P. Cladis and S. Torza, J. Appl. Phys. **46**, 584 (1975).
[17] C. Gooden, R. Mahmood, D. Brisbin, A. Baldwin, D. L. Johnson, and M. E. Neubert, Phys. Rev. Lett. **54**, 1035 (1985).
[18] C. Chevallard and M. G. Clerc, Phys. Rev. E **65**, 011708 (2001).
[19] I. Lelidis and G. Barbero, Europhys. Lett. **61**, 646 (2003).
[20] F. J. Kahn, Appl. Phys. Lett. **22**, 386 (1973).
[21] I. Lelidis, A. Gharby, and G. Durand, Mol. Cryst. Liq. Cryst.

223, 263 (1992).
[22] D. Subacius, V. M. Pergamenshchik, and O. D. Lavrentovich, Mol. Cryst. Liq. Cryst. **288**, 129 (1996).
[23] M. Kléman and C. Williams, Philos. Mag. **28**, 725 (1973).
[24] S. Faetti and M. Riccardi, J. Phys. II **5**, 1165 (1995); V. M. Pergamenshchik and S. Žumer, Phys. Rev. E **59**, R2531 (1999).
[25] Zili Li and O. D. Lavrentovich, Phys. Rev. Lett. **73**, 280 (1994).
[26] N. V. Madhusudana and R. Pratibha, Mol. Cryst. Liq. Cryst. **89**, 249 (1982).